Journal of Robotics and Control (JRC)
Volume 6, Issue 3, 2025
ISSN: 2715-5072, DOI: 10.18196/jrc.v6i3.26318

Fractional Order Extended State Observer Enhances the Accuracy of Estimation for Flexible Joint Single-link Robot

Hakam Marwan [1*], Amjad J. Humaidi [2], Huthaifa Al-Khazraji [3]
[1, 2, 3] Department of Systems and Control Engineering, University of Technology, Baghdad, 10069, Iraq
[1] College of Electronics Engineering, Ninevah University, Mosul, 41002, Iraq
Email: [1] cse.23.15@grad.uotechnology.edu.iq, [2] amjad.j.humaidi@uotechnology.edu.iq, [3] 60141@uotechnology.edu.iq
*Corresponding Author

***Abstract*—This study focuses on analyzing and evaluating the performance of three types of Extended State Observers (ESOs)—Linear ESO (LESO), Nonlinear ESO (NESO), and Fractional-Order ESO (FOESO)—within a flexible joint robotic system. ESOs are a key component of Active Disturbance Rejection Control (ADRC) due to their ability to estimate system states and internal and external disturbances without requiring an accurate system model, making them particularly suitable for nonlinear and complex systems. This research aims to provide a quantitative comparison among the three observer types under parameter uncertainties and external disturbances using MATLAB/SIMULINK simulations. By reducing the RMSE, a Genetic Algorithm (GA) finds the optimal observer parameters. The results indicate that FOESO significantly outperforms the other observers in terms of estimation accuracy, achieving a remarkably low RMSE of 1.06×10^{-16} for position estimation, compared to 9.16×10^{-13} for NESO and 2.17×10^{-11} for LESO. These findings highlight FOESO's superior robustness in managing nonlinearities and disturbances, making it a promising solution for high-precision robotic applications.**

Keywords*—*Flexible Joint System; Extended State Observer; RMSE; Disturbance Rejection; Active Disturbance Rejection Control.

I. INTRODUCTION

Robotics has evolved into a multidisciplinary field that has witnessed remarkable advancements over time, driven by developments in electronics, control theory, system modeling, simulation techniques, brain–machine interfaces, and cognitive sciences. The continuous integration of these technologies has significantly shaped modern robotic research and applications.

The application of robotics has markedly increased. Robots are becoming increasingly vital across diverse domains, including medicine, haptics, nuclear power facilities, space exploration, automation, and industry, as well as in underwater operations, target tracking, and tethering applications. In the medical domain, robotic systems have shown substantial potential in diverse areas such as rehabilitation [23], motion assistance [24]–[25], anesthesia management [26], and the enhancement of patient mobility [27].

The locomotion subsystem of robots mainly consists of links, legs, wheels, or combinations. Consequently, the control community has been involved in proposing creative solutions for mobile robots and link-based operations. Both linear [36]-[37] and non-linear control approaches [38]-[39] have been successfully applied to the ensuing constructions.

Flexible joint systems are a vital area of research in robotics and mechanical engineering. These systems consist of a flexible link connected to an actuator by a flexible joint, affecting the dynamics and control of the entire system [40]. Flexible joint robotic manipulators (FJRMs) have attracted significant research interest due to advancements in the industry and the rising desire for lightweight, energy-efficient robots in modern society. Robotic manipulators are complex, non-linear systems employed across various industries, including beverage production, automotive assembly, aerospace, underwater vehicles, agriculture, automation, and medical applications. FJRMs offer several advantages over traditional heavy-weight and rigid-link robotic manipulators (RRMs), such as reduced size, decreased weight, enhanced maneuverability, improved transportability, lower power consumption, diminished control effort, reduced cost, expansive work volume, increased motion speed, more miniature actuators, and heightened operational velocity due to minimized inertia [46]-[51].

In specific controllers, the control mechanism is classified into two categories: state feedback and output feedback. The output feedback demonstrated by Active Disturbance Rejection Control (ADRC) requires incorporating an observer, making this control method primarily observer-focused [52]-[55]. An observer is a mathematical and technical apparatus employed in contemporary control methodologies to deduce internal state variables from quantifiable inputs and outputs. Improving system performance and monitoring is essential, particularly when certain internal states are unmeasurable. Observer-based control systems have been widely employed in several engineering fields to enhance performance and save costs. To reduce the impact of chatter and vibration, machine tool control observers measure the motion of the cutting tool and the workpiece [56].

Researchers in the literature have utilized several types of observers to assess the states of the FJRMs. In [57], Léchevin proposed the development of two distinct observer designs: (1) a variable structure observer that relies on link

position measurements to estimate the complete state of a flexible joint manipulator, and (2) a reduced-order adaptive observer that requires both link and motor position measurements for accurate state estimation. In [58], Abdollahi presented a stable observer utilizing neural networks for flexible-joint manipulators. In [59], Ullah utilizes the High Gain Observer alongside output feedback control to manage single-link flexible-joint robot manipulators (SFJRMs) in the presence of matched disturbances and parametric uncertainties. In [60], Ma develops an adaptive neural control approach for n-link flexible-joint electrically driven robots, utilizing an adaptive observer to forecast the velocities of the links and motors. In [61], Talole proposed a feedback linearization (FL)-based control law, executable via an extended state observer (ESO), for the trajectory tracking control of a flexible-joint robotic system. Bortoff suggests a resilient observer-based control technique for flexible joint robots [58].

This paper proposes an extended state observer (ESO) to estimate the states of Flexible Joint Robotic Manipulators (FJRMs), considering the lumped uncertainty present in the system. This observer signifies a fresh methodology, differing from those previously documented in the literature, save for the study of Talole [61]. An optimization technique is established to ascertain the observer gain values, and a novel observer, the Fractional-Order Extended State Observer (FOESO), is presented. A comparative examination is performed among the three types of ESO. The calculated states encompass the angular location, velocity, acceleration, and jerk of the FJRMs, while the observer also assesses the total uncertainties stemming from external disturbances and nonlinearities in spring characteristics. The research examines three variants of the Extended State Observer (ESO): the Linear Extended State Observer (LESO), the Nonlinear Extended State Observer (NESO), and the Fractional-Order Extended State Observer (FOESO). These principal contributions can be encapsulated as follows:

- The design of LESO, NESO, and FOESO.
- A comparative performance assessment of LESO, NESO, and FOESO utilizing the Root Mean Square Error (RMSE) statistic.

II. MATHEMATICAL MODEL

In this work, a mathematical model is presented for a single-link manipulator with a revolute joint, actuated by a DC motor. The flexibility of the joint is modeled as a linear torsional spring with stiffness K, as illustrated in Fig. 1.

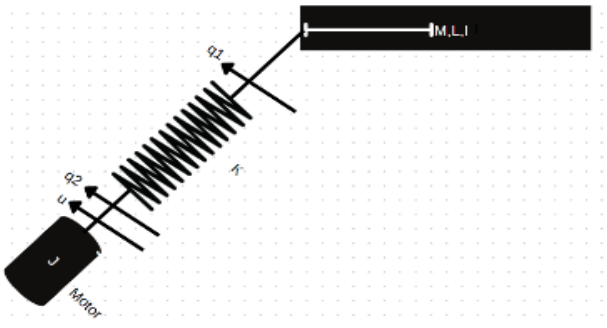

Fig. 1. Flexible-joint manipulator system

The equations of motion for this system [63] are given by:

$$\begin{aligned} I\ddot{q}_1 + MgLsin(q_1) + K(q_1 - q_2) = 0 \\ J\ddot{q}_2 - K(q_1 - q_2) = u \end{aligned} \quad (1)$$

For this context, q_1 and q_2 are the link and motor angles, I and J are the link and motor inertia, K and u are the spring stiffness and input torque, and M and L are the mass and length of the link, respectively. Designating the state variables as $x_1 = q_1, x_2 = \dot{q}_1, x_3 = q_2, x_4 = \dot{q}_2$. The nonlinear dynamics (1) can be expressed in a state space model as:

$$\begin{aligned} \dot{x}_1 &= x_2 \\ \dot{x}_2 &= -\frac{MgL}{I} sin(x_1) - \frac{K}{I}(x_1 - x_3) \\ \dot{x}_3 &= x_4 \\ \dot{x}_4 &= \frac{K}{J}(x_1 - x_3) + \frac{1}{J}u \end{aligned} \quad (2)$$

The system's output can be described as:

$$y = h(x) = x_1 \quad (3)$$

It should be noted that a nonlinear system can be turned into the "normal form" of interest by making the right changes to the coordinates in the state space. In this form, many important aspects can be revealed. None of the three equations in the nonlinear dynamic system (1) are in standard form. A nonlinear coordinate transformation will normalize the system and simplify the control design. Using the form's nonlinear coordinate transformation on it. Using the converted new coordinates, one can rewrite the unique dynamics (1)–(3) as:

$$Z = \begin{bmatrix} L_f^0 h \\ L_f^1 h \\ L_f^2 h \\ L_f^{n-1} h \end{bmatrix} \quad (4)$$

The $L_f h(x) = \frac{\partial(h)}{\partial x} f(x)$ Lie derivatives of the system.

$$\begin{aligned} z_1 = h(x) &= x_1 \\ z_2 = L_f^1 h &= x_2 \\ z_3 = L_f^2 h &= -\frac{MgL}{I} sin(x_1) - \frac{K}{I}(x_1 - x_3) \\ z_4 = L_f^3 h &= -\frac{MgL}{I} cos(x_1)x_2 - \frac{K}{I}(x_2 - x_4) \end{aligned} \quad (5)$$

Being a global diffeomorphism, the transformation z=T(x) is a smooth, bijective mapping with a smooth inverse. This preserves the smoothness of the original system and guarantees a clear definition of the changed coordinates. The changed variables z1, z2, z3, and z4 match, respectively, the position, velocity, acceleration, and jerk of the connection, as reported. Consequently, reformulating the original dynamics (2)-(3) concerning these new coordinates helps to simplify analysis and control design.

$$\begin{aligned} \dot{z}_1 &= z_2 \\ \dot{z}_2 &= z_3 \\ \dot{z}_3 &= z_4 \\ \dot{z}_4 &= a(z) + bu \end{aligned} \quad (6)$$

where a(z) (all the non-linearized) and b are given by:

$$a(z) = \frac{MgL}{I} sin(z_1)\left({z_2}^2 - \frac{K}{J}\right) - \left(\frac{MgL}{I} cos(z_1) + \frac{K}{J} + \frac{K}{I}\right) z_3$$

$$b = \frac{k}{IJ}$$

III. ESO DESIGN

An observer, an ESO, can determine a system's uncertainties and states, enabling it to compensate for or reject disruptions. It treats uncertainties, nonlinear dynamics, coupling effects, and external disturbances as full-blown disturbances. Regardless of the plant's mathematical model, ESO is easier to implement and produces superior results. In many different domains, it finds use. The LESO, NLESO, and FESO approach is laid forth in this research. Here is an explanation of ESO's fundamental idea:

Consider an n^{th}order, single single-output nonlinear dynamical system described by:

$$z^{(n)} = a(z, \dot{z}, \dots, z_{n+1}, w) + bu \tag{7}$$

According to equation (7), a (.) denotes the plant dynamics, u signifies the control signal, z represents the measured output, and w(t) indicates an unknown disturbance. Furthermore, a (.) is expressed as a_o (.) + Δ a, and b is defined as b_0 + Δb, where a_o (.) and b_o These are the most accurate estimates of $a_o$and b_o, respectively, while Δ a and Δb denotes their corresponding uncertainties in Equation (7) can be reformulated in state-space representation by defining the uncertainty as d≡Δa+Δbu and identifying it as an extended state, z_{n+1}The dynamics (7) can be expressed in state-space representation as:

$$\begin{aligned} \dot{z}_1 &= z_2 \\ \dot{z}_2 &= z_3 \\ &\vdots \\ \dot{z}_n &= z_{n+1} + a_o + b_o u \\ \dot{z}_{n+1} &= h \\ y &= z_1 \end{aligned} \tag{8}$$

The uncertainty's rate of change, denoted as h=$\dot{d}$, is a bounded, unknown function that can be estimated using a state estimator once d is transformed into a state.

A. Linear Extended State Observer

It is the simplest type of ESO. The equations of LESO are given in equation (9).

$$\begin{aligned} \dot{\hat{z}}_1 &= \hat{z}_2 + \beta_1(e) \\ \dot{\hat{z}}_2 &= \hat{z}_3 + \beta_2(e) \\ &\vdots \\ \dot{\hat{z}}_n &= \hat{z}_{n+1} + \beta_n(e) + b_o u \\ \dot{\hat{z}}_{n+1} &= \beta_{n+1}(e) \end{aligned} \tag{9}$$

Where $e = y - \hat{z}_1$.The observer's states $(z_1, .., z_n)$ work to estimate the actual states of the system $(x_1, \dots, x_n)$ respectively, while the state of the observer z_{n+1} is responsible for estimating the lumped uncertainties h(x). The parameters $[\beta_1, .., \beta_{n+1}]$ are positive constants. The values of the coefficients are determined using optimization methods to verify that a given polynomial is Hurwitz. In this context, a Genetic Algorithm (GA) will be utilized as the optimization technique to find the appropriate coefficient values, ensuring that the polynomial satisfies the Hurwitz criterion. Meaning all its roots have negative real parts. the following goal from the designed observer $z_1 \longrightarrow x_1$, $z_2 \longrightarrow x_2, z_3 \longrightarrow x_3, z_4 \longrightarrow x_4, z_5 \longrightarrow h(x)$as $t \longrightarrow \infty$.

B. Nonlinear Extended State Observer

The second version of ESO is NESO. This type is considered more complex than the first version because it contains more variables. NESO type can be expressed by the following equations (10).

$$\begin{aligned} \dot{\hat{z}}_1 &= \hat{z}_2 + \beta_1 g_1(e) \\ \dot{\hat{z}}_2 &= \hat{z}_3 + \beta_2 g_2(e) \\ &\vdots \\ \dot{\hat{z}}_n &= \hat{z}_{n+1} + \beta_n g_n(e) + b_o u \\ \dot{\hat{z}}_{n+1} &= \beta_{n+1} g_{n+1}(e) \end{aligned} \tag{10}$$

Where $e = y - \hat{z}_1$ and $\hat{z}_{n+1}$ It is an estimate of the uncertainty. The quantities are the observer gains, while g_i(.) are the set of suitably constructed nonlinear gain functions that are satisfying $e g_i(e) > 0, \forall e \neq 0$ and $g_i(0) = 0$. If one chooses the nonlinear functions, g_i(.) and their related parameters are properly estimated, it is anticipated that the estimated state variables $\hat{z}_i$ converge to the corresponding system states. z_i, i.e., $\hat{z}_i \rightarrow z_i$; i=1, 2…, n+1. An essential component of ESO design is the selection of the nonlinear function. These functions' general formulation was chosen empirically based on experimental findings [64-67] is

$$g_i(e, \alpha_i, \delta) = \begin{cases} |e|^{\alpha_i} \text{sign}(e), & |e| > \delta \\ \dfrac{e}{\delta^{1-\alpha_i}}, & |e| \leq \delta \end{cases} \quad i = 1,2, \dots, n+1 \tag{11}$$

where δ is greater than zero. As can be seen, g_i(.) is a nonlinear function with a linear interval close to the origin. Avoid going close to the origin. One crucial characteristic of these functions is that for $0<\alpha_i<1$. The function g_i *(.)* generates a small gain when the error is large and a significant gain when the error is minor, with the benefit being limited by a small constant. The error range corresponds to high gain and is established in the vicinity of the origin.

C. Fractional Order Extended State Observer

The remaining version of ESO, Fractional-order extended country observers (FOESO) have shown promising results in diverse control packages. They offer advanced performance and higher estimation accuracy compared to integer-order observers [68]-[70]. An extension of integration and differentiation to a non-integer order operator is the fractional calculus:

$$D^{\alpha} = \begin{cases} \frac{d^{\alpha}}{d_t^{\alpha}} & for\ \alpha \succ 0 \\ 1 & for\ \alpha = 0 \\ \int_a^t (dt)^{-\alpha} & for\ \alpha \prec 0 \end{cases} \tag{12}$$

The fractional order (α) ranges from 0 to 1, and a and t represent the operation's limitations, allowing for the derivative in all estimate states of the observer. $\hat{x} = [\hat{x}_1, \hat{x}_2, \dots \dots, \hat{x}_n, \hat{x}_{n+1}]$. Expresses equations of this type.

$$\begin{aligned} D^{\alpha_f}\hat{x}_1 &= \hat{x}_2 + \beta_1(y - \hat{x}_1) \\ D^{\alpha_f}\hat{x}_2 &= \hat{x}_3 + \beta_2(y - \hat{x}_1) \\ D^{\alpha_f}\hat{x}_n &= \hat{x}_{n+1} + bu + \beta_n(y - \hat{x}_1) \\ D^{\alpha_f}\hat{x}_{n+1} &= \beta_{n+1}(y - \hat{x}_1) \\ \hat{y}_1 &= c\hat{x}_1 \end{aligned} \tag{13}$$

The parameters α and observer's gains $[\beta_1, . \beta_{n+1},]$ are positive

IV. RESULTS AND DISCUSSION

Three observer classifications—LESO, NESO, and FOESO—were evaluated using MATLAB/Simulink via a numerical simulation. Thanks to its connection with strong analytical and computational tools, this platform has enormous possibilities in system monitoring, control, and other technical disciplines. The recommended tool for precisely running complex computations and differential equation solutions is MATLAB/Simulink. Moreover, it provides a lot of programming freedom so control engineers can create MATLAB scripting, Simulink block diagrams, or integrated control algorithms. This adaptability enables one to create exact models of dynamic systems and build control rules. Table I lists the physical parameters of the flexible joint system applicable to all kinds of observers.

TABLE I. PARAMETERS OF THE MAGLEV SYSTEM

Parameters	Values
MgL	10N−m
K	100N−m/rad
I	1kg−m2
J	1kg−m2
input	Sin(t)
X (0)	[0 0 0 0]
Z (0)	[0 0 0 0 0]

The Genetic Algorithm (GA) is applied to the three types of Extended State Observer (ESO) to decrease the Root Mean Squared Error (RMSE) as the objective feature, as given in Eq. (14) [71]-[73].

$$RMSE = \sqrt{\frac{\sum_{i=1}^{N} \|x(i) - \hat{x}(i)\|^2}{N}} \quad (14)$$

The effects verified that the usage of GA significantly advanced estimation accuracy and reduced errors caused by outside disturbances and system uncertainties. The optimization process was conducted with the following GA parameters of:

- Number of generations**:** *25*
- Population size: *50*

The range of the design variables of each observer is given in Table II, Table III, and Table IV. The best value of each observer is given in Table V.

TABLE II. THE UPPER AND LOWER OF LESO

Parameter	Lower bound	Upper bound
$\beta_1, \beta_2, \beta_3, \beta_4, \beta_5$	0	10^{18}

TABLE III. THE UPPER AND LOWER OF NESO

Parameter	Lower bound	Upper bound
$\beta_1, \beta_2, \beta_3, \beta_4, \beta_5$	0	10^{18}
$\alpha_1, \alpha_2, \alpha_3, \alpha_4, \alpha_5$	0	1

TABLE IV. THE UPPER AND LOWER OF FOESO

Parameter	Lower bound	Upper bound
$\beta_1, \beta_2, \beta_3, \beta_4, \beta_5$	0	10^{18}
$\alpha_1, \alpha_2, \alpha_3, \alpha_4, \alpha_5$	0	1
δ	0	0.5

TABLE V. THE OUTPUT OF GA PARAMETERS

Typer of ESO	Parameter	Value
LESO	β_1	$1.25 * 10^3$
	β_2	799368
	β_3	$1.28 * 10^8$
	β_4	$1.62 * 10^{10}$
	β_5	$9.48 * 10^{11}$
NESO	β_1	$2.079 * 10^3$
	β_2	$8.87 * 10^5$
	β_3	$2.345 * 10^8$
	β_4	$3.77 * 10^{10}$
	β_5	$2.59 * 10^{11}$
	δ	0.107
	α_1	0.998
	α_2	0.5
	α_3	0.25
	α_4	0. 125
	α_5	0.0625
FOESO	β_1	$1.4 * 10^4$
	β_2	$5.52 * 10^7$
	β_3	$1.68 * 10^{11}$
	β_4	$3.34 * 10^{14}$
	β_5	$1.91 * 10^{17}$
	α_1	0.9979
	α_2	0.9974
	α_3	0.9930
	α_4	0.9955
	α_5	0.9890

The flexible joint system's actual and estimated states and uncertainties are shown in Fig. 2, Fig. 3, and Fig. 4, respectively, utilizing LESO, NESO, and FOESO. The corresponding RMSE-based performance evaluations for each type of ESO are included in Table VI, Table VII, and Table VIII.

TABLE VI. RMSE OF THE ESTIMATION ERROR OF THE LESO

Estimation Error	**RMSE**
$x_1 - \hat{x}_1$	2.1749e-11
$x_2 - \hat{x}_2$	2.7330e-08
$x_3 - \hat{x}_3$	1.7361e-05
$x_4 - \hat{x}_4$	0.0028
$x_5 - \hat{x}_5$	0.3499

TABLE VII. RMSE OF THE ESTIMATION ERROR OF THE NESO

Estimation Error	**RMSE**
$x_1 - \hat{x}_1$	9.1624e-13
$x_2 - \hat{x}_2$	1.9046e-09
$x_3 - \hat{x}_3$	2.5694e-06
$x_4 - \hat{x}_4$	0.0012
$x_5 - \hat{x}_5$	0.2585

TABLE VIII. RMSE OF THE ESTIMATION ERROR OF THE FOESO

Estimation Error	**RMSE**
$x_1 - \hat{x}_1$	1.0632e-16
$x_2 - \hat{x}_2$	2.1190e-05
$x_3 - \hat{x}_3$	1.0303e-05
$x_4 - \hat{x}_4$	6.8519e-04
$x_5 - \hat{x}_5$	0.0429

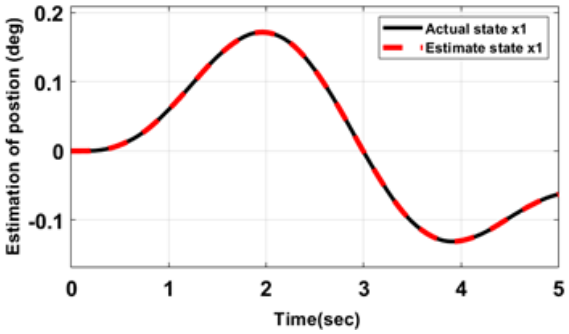

(a)

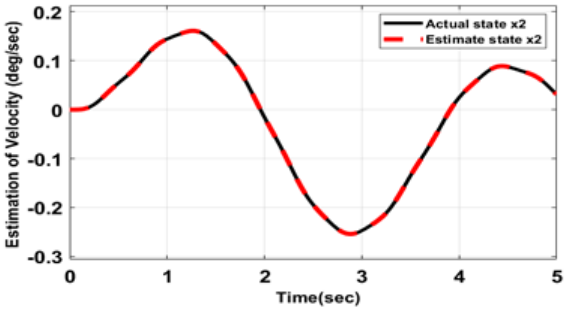

(b)

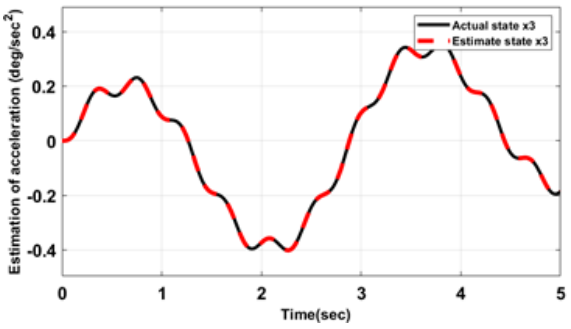

(c)

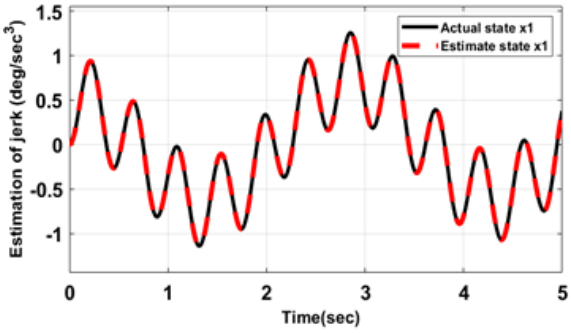

(d)

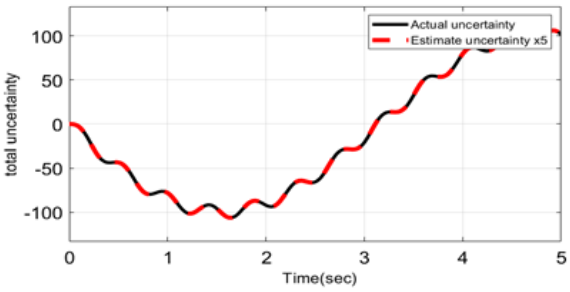

(e)

Fig. 2. The output of LESO: a) angular position, b) angular velocity, c) angular acceleration, d) jerk, e) total uncertainty

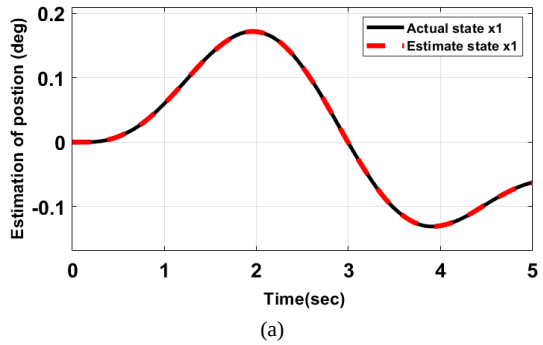

(a)

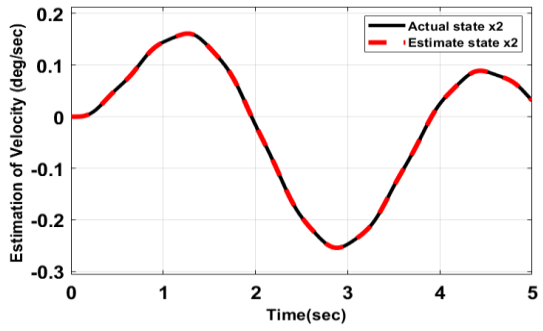

(b)

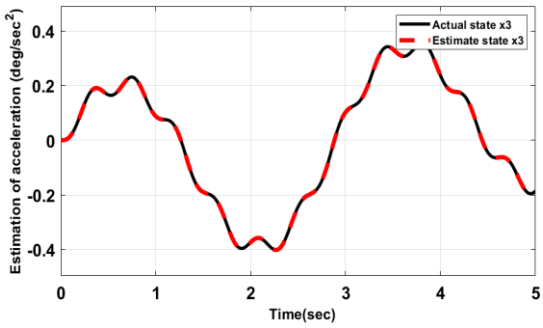

(c)

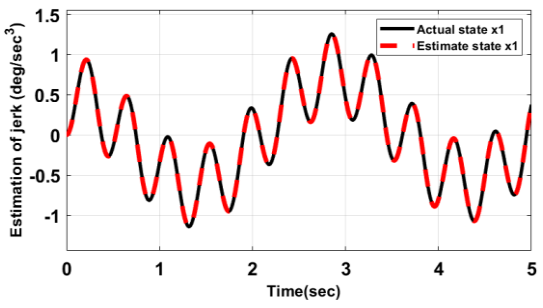

(d)

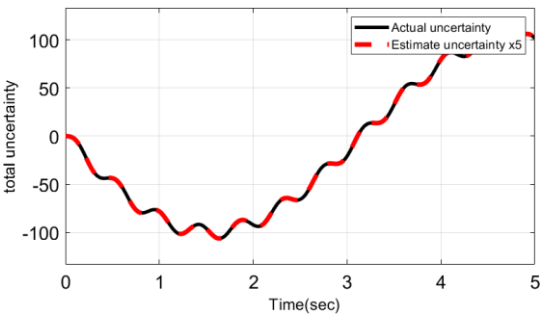

(e)

Fig. 3. The output of NESO: a) angular position, b) angular velocity, c) angular acceleration, d) jerk, e) total uncertainty

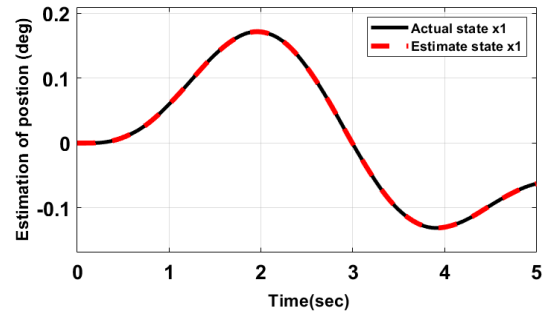

(a)

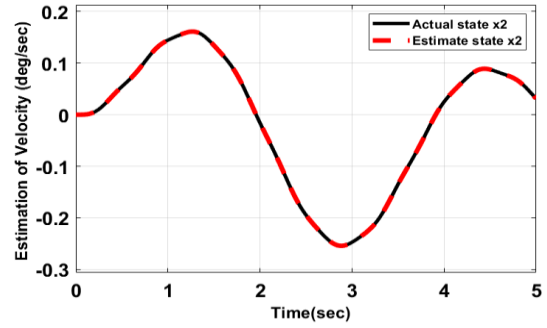

(b)

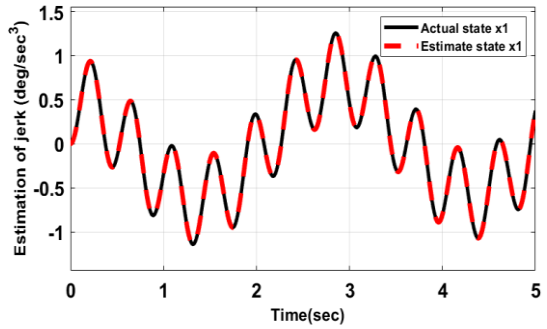

(c)

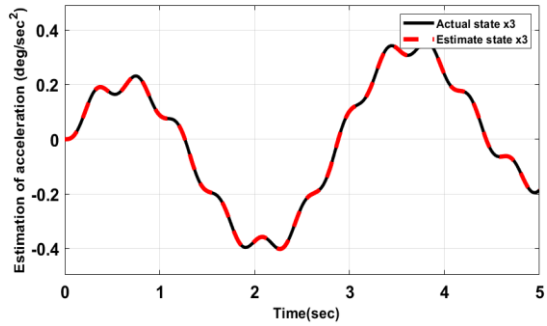

(d)

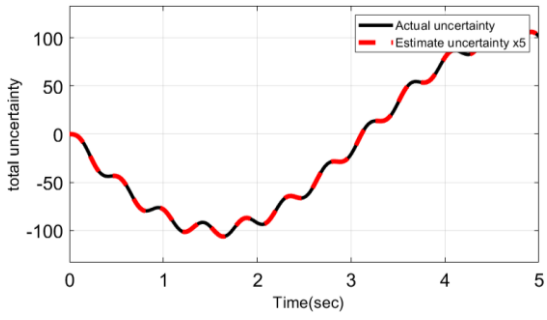

(e)

Fig. 4. The output of FOESO: a) angular position, b) angular velocity, c) angular acceleration, d) jerk, e) total uncertainty

The most important estimating the error is the state x_1 because it is the output of the system. For comparison, it can be seen from Fig. 5 that FOESO is better than the rest because it has the lowest RMSE value than the rest, then NESO comes in second place, and the last one is LESO. The second thing we will compare is which one is better at assessing uncertainty and which one is less valuable. Based on Fig. 6, it is clear to us that FOSEO is also better than the rest, NESO comes in second, and LESO comes last. We conclude from these results that the FOESO is the best type that can be used for the flexible joint system.

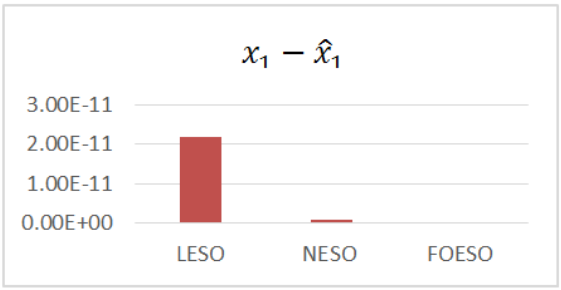

Fig. 5. Estimating the error of x_1 for LESO, NESO and FPSEO

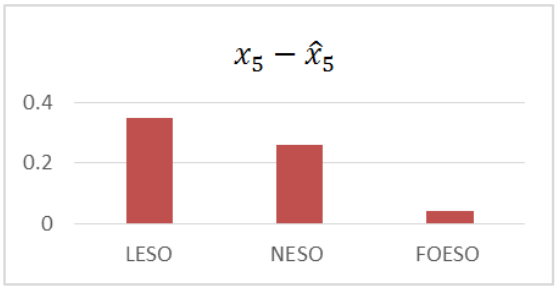

Fig. 6. Estimating the error of x_5 for LESO, NESO and FPSEO

V. CONCLUSION

Three different Extended State Observers (ESOs)—LESO, NESO, and FOESO—were evaluated in this comparative study for their ability to estimate the states and uncertainty of flexible joint robotic systems. All observer versions accomplished reliable state tracking using MATLAB/SIMULINK simulations and optimization based on Genetic Algorithm (GA). Compared to its competitors, FOESO achieved the best results regarding angular position and uncertainty estimation, as measured by Root Mean Square Error (RMSE). Additionally, NESO demonstrated its capacity to deal with nonlinear dynamics by producing dependable results. On the other hand, LESO showed greater estimating mistakes, notwithstanding its effectiveness. The results show that FOESO is the best solution for real-time control applications in flexible joint systems, especially when optimized with GA. It is robust and precise. This study concludes that fractional-order techniques should be implemented in modern control frameworks to improve system performance, resilience to disruptions, and estimation accuracy.

REFERENCES

[1] S. A. Ajwad and J. Iqbal, "Emerging trends in robotics—A review from applications perspective," in *Proc. Int. Conf. Eng. Emerg. Technol. (ICEET)*, pp. 1–6, 2015.

[2] J. Iqbal *et al*., "ARM solutions for text, audio and image data processing for ultra low power applications," in *Proc. IEEE Int. Multitopic Conf*., pp. 32–35, 2004.

[3] M. F. Khan, R. U. Islam, and J. Iqbal, "Control strategies for robotic manipulators," in *Proc. IEEE Int. Conf. Robot. Artif. Intell. (ICRAI)*, pp. 26–33, 2012.

[4] M. I. Ullah *et al*., "Modeling and computed torque control of a 6 degree of freedom robotic arm," in *Proc. IEEE Int. Conf. Robot. Emerg. Allied Technol. Eng.*, pp. 133–138, 2014.

[5] A. Meddahi *et al*., "API based graphical simulation of robotized sites," in *Proc. 14th IASTED Int. Conf. Robot. Appl.*, pp. 485–492, 2009.

[6] K. Naveed and J. Iqbal, "Brain controlled human robot interface," in *Proc. IEEE Int. Conf. Robot. Artif. Intell.*, pp. 55–60, 2012.

[7] M. M. Azeem *et al*., "Emotions in robots," in *Emerging Trends Appl. Inf. Commun. Technol*., vol. 281, pp. 144–153, 2012.

[8] J. Iqbal *et al*., "Automating industrial tasks through mechatronic systems—A review of robotics in industrial perspective," *Tech. Gaz.*, vol. 23, no. 3, pp. 917–924, 2016.

[9] J. Iqbal and K. Baizid, "Stroke rehabilitation using exoskeleton-based robotic exercisers: Mini review," *Biomed. Res.*, vol. 26, no. 2, pp. 197–201, 2015.

[10] J. Iqbal, N. Tsagarakis, and D. Caldwell, "Four-fingered lightweight exoskeleton robotic device accommodating different hand sizes," *Electron. Lett.*, vol. 51, no. 12, pp. 888–890, 2015.

[11] J. Iqbal, O. Ahmad, and A. Malik, "HEXOSYS II—Towards realization of light mass robotics for the hand," in *Proc. 14th IEEE Int. Multitopic Conf.*, pp. 115–119, 2011.

[12] J. Iqbal and A. M. Tahir, "Robotics for nuclear power plants—Challenges and future perspectives," in *Proc. 2nd IEEE Int. Conf. Appl. Robot. Power Ind.*, pp. 151–156, 2012.

[13] J. Iqbal *et al*., "State estimation technique for a planetary robotic rover," *Rev. Fac. Ing. Univ. Antioquia*, no. 70, pp. 58–68, 2014.

[14] J. Iqbal, S. Heikkilä, and A. Halme, "Tether tracking and control of ROSA robotic rover," in *Proc. 10th IEEE Int. Conf. Control, Autom., Robot. Vis.*, pp. 689–693, 2008.

[15] J. Iqbal *et al*., "A novel track-drive mobile robotic framework for conducting projects on robotics and control systems," *Life Sci. J.*, vol. 10, no. 2, pp. 130–137, 2013.

[16] K. Baizid *et al*., "Modelling of robotized site and simulation of robots' optimum placement and orientation zone," in *Proc. 21st IASTED Int. Conf. Model. Simul.*, pp. 9–16, 2010.

[17] K. Baizid *et al*., "Time scheduling and optimization of industrial robotized tasks based on genetic algorithms," *Robot. Comput.-Integr. Manuf.*, vol. 34, pp. 140–150, 2015.

[18] K. Baizid *et al*., "Robotized task time scheduling and optimization based on Genetic Algorithms for non redundant industrial manipulators," in *Proc. IEEE Int. Symp. Robot. Sens. Environ.*, pp. 112–117, 2014.

[19] A. M. Tahir and J. Iqbal, "Underwater robotic vehicles: Latest development trends and potential challenges," *Sci. Int.*, vol. 26, no. 1, pp. 1–5, 2014.

[20] J. Iqbal *et al*., "Real-time target detection and tracking: A comparative in-depth review of strategies," *Life Sci. J.*, vol. 10, no. 3, pp. 804–813, 2013.

[21] J. Iqbal *et al*., "Computer vision inspired real-time autonomous moving target detection, tracking and locking," *Life Sci. J.*, vol. 10, no. 4, pp. 3338–3345, 2013.

[22] S. A. Ajwad and J. Iqbal, "Recent advances and applications of tethered robotic systems," *Sci. Int.*, vol. 26, no. 4, pp. 2045–2051, 2014.

[23] J. Iqbal, N. Tsagarakis, and D. Caldwell, "Design optimization of a hand exoskeleton rehabilitation device," in *Proc. RSS Workshop Understand. Hum. Hand Adv. Robot. Manip.*, pp. 44–45, 2009.

[24] J. Iqbal, N. Tsagarakis, and D. Caldwell, "Human hand compatible underactuated exoskeleton robotic system," *Electron. Lett.*, vol. 50, no. 7, pp. 494–496, 2014.

[25] J. Iqbal *et al*., "Design requirements of a hand exoskeleton robotic device," in *Proc. 14th IASTED Int. Conf. Robot. Appl.*, pp. 44–51, 2009.

[26] I. Muhammad *et al*., "Regulation of hypnosis in Propofol anesthesia administration based on non-linear control strategy," *Braz. J. Anesthesiol.*, vol. 66, no. 4, pp. 367–375, 2016.

[27] A. A. Khan, R. U. Nabi, and J. Iqbal, "Surface estimation of a pedestrian walk for outdoor use of power wheel chair based robot," *Life Sci. J.*, vol. 10, no. 4, pp. 1697–1704, 2013.

[28] M. I. Ullah *et al.*, "Non-linear control law for articulated serial manipulators: Simulation augmented with hardware implementation," *Electron. Electr. Eng.*, vol. 22, no. 2, pp. 3–7, 2016.

[29] O. Ahmad, I. Ullah, and J. Iqbal, "A multi-robot educational and research framework," *Int. J. Acad. Res.*, vol. 6, no. 1, pp. 217–222, 2014.

[30] M. Zohaib *et al*., "An improved algorithm for collision avoidance in environments having U and H shaped obstacles," *Stud. Inform. Control*, vol. 23, no. 1, pp. 97–106, 2014.

[31] M. Zohaib *et al*., "Addressing collision avoidance and nonholonomic constraints of a wheeled robot: Modeling and simulation," in *Proc. IEEE Int. Conf. Robot. Emerg. Allied Technol. Eng.*, pp. 306–311, 2014.

[32] R. U. Nabi *et al*., "A unified SLAM solution using partial 3D structure," *Electron. Electr. Eng.*, vol. 20, no. 2, pp. 3–8, 2014.

[33] M. Zohaib *et al*., "IBA: Intelligent Bug Algorithm—A novel strategy to navigate mobile robots autonomously," in *Emerging Trends Appl. Inf. Commun. Technol.*, vol. 281, pp. 291–299, 2013.

[34] A. H. Arif *et al*., "A hybrid humanoid-wheeled mobile robotic educational platform—Design and prototyping," *Indian J. Sci. Technol.*, vol. 7, no. 10, pp. 2140–2148, 2015.

[35] H. Khan *et al*., "Longitudinal and lateral slip control of autonomous wheeled mobile robot for trajectory tracking," *Front. Inf. Technol. Electron. Eng.*, vol. 16, no. 2, pp. 166–172, 2015.

[36] S. A. Ajwad, U. Iqbal, and J. Iqbal, "Hardware realization and PID control of multi-degree of freedom articulated robotic arm," *Mehran Univ. Res. J. Eng. Technol.*, vol. 34, no. 1, pp. 1–12, 2015.

[37] U. Iqbal *et al*., "Embedded control system for AUTAREP—A novel AUTonomous Articulated Robotic Educational Platform," *Tech. Gaz.*, vol. 21, no. 6, pp. 1255–1261, 2014.

[38] J. Iqbal *et al*., "Towards sophisticated control of robotic manipulators: An experimental study on a pseudo-industrial arm," *Stroj. Vestn.-J. Mech. Eng.*, vol. 61, no. 7–8, pp. 465–470, 2015.

[39] S. A. Ajwad *et al*., "Disturbance-observer-based robust control of a serial-link robotic manipulator using SMC and PBC techniques," *Stud. Inform. Control*, vol. 24, no. 4, pp. 401–408, 2015.

[40] F. Xi and R. G. Fenton, "Coupling effect of a flexible link and a flexible joint," *Int. J. Robot. Res.*, vol. 13, no. 5, pp. 443–453, 1994.

[41] S. Ulrich, J. Z. Sasiadek, and I. Barkana, "Nonlinear adaptive output feedback control of flexible-joint space manipulators with joint stiffness uncertainties," *J. Guid., Control, Dyn.*, vol. 37, no. 6, pp. 1961–1975, 2014.

[42] L. Qiao and W. Zhang, "Adaptive non-singular integral terminal sliding mode tracking control for autonomous underwater vehicles," *IET Control Theory Appl.*, vol. 11, no. 8, pp. 1293–1306, 2017.

[43] A. Suprem, N. Mahalik, and K. Kim, "A review on application of technology systems, standards and interfaces for agriculture and food sector," *Comput. Stand. Interfaces*, vol. 35, no. 4, pp. 355–364, 2013.

[44] C. Yang *et al*., "Global adaptive tracking control of robot manipulators using neural networks with finite-time learning convergence," *Int. J. Control Autom. Syst.*, vol. 15, no. 5, pp. 1916–1924, 2017.

[45] C. Yang *et al*., "Haptic identification by ELM-controlled uncertain manipulator," *IEEE Trans. Syst., Man, Cybern., Syst.*, vol. 47, no. 8, pp. 2394–2409, 2017.

[46] M. Mosayebi, M. Ghayour, and M. J. Sadigh, "A nonlinear high gain observer based input–output control of flexible link manipulator," *Mech. Res. Commun.*, vol. 86, pp. 4–12, 2017.

[47] H. Rahimi and M. Nazemizadeh, "Dynamic analysis and intelligent control techniques for flexible manipulators: A review," *Adv. Robot.*, vol. 28, no. 2, pp. 63–76, 2014.

[48] Z. Chen, M. Wang, and Y. Zou, "Dynamic learning from adaptive neural control for flexible joint robot with tracking error constraints using high-gain observer," *Syst. Sci. Control Eng.*, vol. 6, no. 2, pp. 177–190, 2018.

[49] S. K. Dwivedy and P. Eberhard, "Dynamic analysis of flexible manipulators, a literature review," *Mech. Mach. Theory*, vol. 41, no. 7, pp. 749–777, 2006.

[50] D. Feliu-Talegon *et al*., "Stable force control and contact transition of a single link flexible robot using a fractional-order controller," *ISA Trans.*, vol. 89, pp. 139–157, 2019.

[51] K. Wei and B. Ren, "A method on dynamic path planning for robotic manipulator autonomous obstacle avoidance based on an improved RRT algorithm," *Sensors*, vol. 18, no. 571, 2018.

[52] N. A. Alawad, A. J. Humaidi, and A. S. Alaraji, "Sliding mode-based active disturbance rejection control of assistive exoskeleton device for rehabilitation of disabled lower limbs," *An. Acad. Bras. Cienc.*, vol. 95, no. 2, p. e20220680, Jun. 2023.

[53] A. Q. Al-Dujaili, A. F. Hasan, A. J. Humaidi, and A. Al-Jodah, "Anti-disturbance control design of exoskeleton knee robotic system for rehabilitative care," *Heliyon*, vol. 10, no. 9, p. e28911, 2024.

[54] N. A. Alawad, A. J. Humaidi, A. S. M. Al-Obaidi, and A. S. Alaraji, "Active disturbance rejection control of wearable lower-limb system based on reduced ESO," *Indones. J. Sci. Technol.*, vol. 7, no. 2, pp. 203–218, 2022.

[55] N. A. Alawad, A. J. Humaidi, and A. S. Al-Araji, "Improved active disturbance rejection control for the knee joint motion model," *Math. Model. Eng. Probl.*, vol. 9, no. 2, pp. 477–483, 2022.

[56] E. E. Mitchell and E. Harrison, "Design of a Hardware Observer for Active Machine Tool Control," *Journal of Dynamic Systems Measurement and Control-transactions of The Asme*, vol. 99, pp. 227-232, 1977.

[57] N. Léchevin and P. Sicard, "Observer design for flexible joint manipulators with parameter uncertainties," *Proceedings of International Conference on Robotics and Automation*, vol. 3, pp. 2547-2552, 1997.

[58] F. Abdollahi, H. A. Talebi, and R. V. Patel, "A stable neural network-based observer with application to flexible-joint manipulators," *IEEE transactions on neural networks*, vol. 17, no. 1, pp. 118–129, 2006.

[59] H. Ullah, F. M. Malik, A. Raza, N. Mazhar, R. Khan, A. Saeed, and I. Ahmad, "Robust Output Feedback Control of Single-Link Flexible-Joint Robot Manipulator with Matched Disturbances Using High Gain Observer," *Sensors*, vol. 21, no. 9, p. 3252, 2021.

[60] H. Ma, H. Ren, Q. Zhou, H. Li, and Z. Wang, "Observer-Based Neural Control of N-Link Flexible-Joint Robots," *IEEE Transactions on Neural Networks and Learning Systems*, vol. 35, no. 4, pp. 5295–5305, 2024.

[61] S. E. Talole, J. P. Kolhe, and S. B. Phadke, "Extended-State-Observer-Based Control of Flexible-Joint System with Experimental Validation," *IEEE Trans. Ind. Electron.*, vol. 57, pp. 1411–1419, 2009.

[62] S. A. Bortoff, J. Y. Hung, and M. Spong, "A Discrete-Time Observer for Flexible-Joint Manipulators," in *Proc. of the 28th IEEE Conference on Decision and Control*, vol. 3, pp. 2078-2082, 1989.

[63] M. W. Spong and M. Vidyasagar, *Robot Dynamics and Control*, New York, USA: Wiley, 1989.

[64] W. Wang and Z. Gao, "A Comparison Study of Advanced State Observer Design Techniques," in *Proc. of the American Control Conference*, pp. 4754–4759, Jun. 2003.

[65] A. J. Humaidi and I. K. Ibraheem, "Speed control of permanent magnet DC motor with friction and measurement noise using novel nonlinear extended state observer-based anti-disturbance control," *Energies*, vol. 12, no. 9, p. 1651, 2019.

[66] W. R. Abdul-Adheem, A. T. Azar, I. K. Ibraheem, and A. J. Humaidi, "Novel active disturbance rejection control based on nested linear extended state observers," *Appl. Sci.*, vol. 10, no. 12, p. 4069, 2020.

[67] M. Y. Hassan, A. J. Humaidi, and M. K. Hamza, "On the design of backstepping controller for acrobot system based on adaptive observer," *Int. Rev. Electr. Eng.*, vol. 15, no. 4, pp. 328–335, 2020.

[68] A. Ma'Bdeh, N. Tawalbeh, and R. El-Khazali, "Sensorless Speed Control of a PMSM Using Fractional-Order Extended State Observer," in *2023 International Conference on Fractional Differentiation and Its Applications (ICFDA)*, pp. 1-5, 2023.

[69] A. F. Hasan, A. J. Humaidi, A. S. M. Al-Obaidi, A. K. Al-Mhdawi, and F. A. Abdulmajeed, "Fractional order extended state observer enhances the performance of controlled tri-copter UAV based on active disturbance rejection control," *Stud. Comput. Intell.*, vol. 1090, pp. 439–487, 2023.

[70] A. H. Hameed, S. A. Al-Samarraie, and A. J. Humaidi, "Backstepping-based nonlinear disturbance observer for speed control of DC motor," *AIP Conf. Proc.*, vol. 3232, no. 1, p. 030007, 2024.

[71] I. Toumi, B. Meghni, O. Hachana, G. Fusco, and N. K. Bahgaat, "Robust variable-step perturb-and-observe sliding mode controller for grid-connected wind-energy-conversion systems," *Entropy*, vol. 24, no. 5, p. 731, 2022.

[72] A. J. Humaidi, A. A. Mohammed, A. H. Hameed, A. T. Azar, and A. Q. Al-Dujaili, "State estimation of rotary inverted pendulum: A comparative study of observers performance," *2020 IEEE Congreso Bienal de Argentina, ARGENCON 2020*, pp. 9505507, 2020.

[73] A. J. Humaidi, E. N. Tala'at, A. Q. Al-Dujaili, D. A. Pereira, and I. K. Ibraheem, "Design of backstepping control based on adaptive observer for underactuated system," *7th Int. Conf. Control, Decis. Inf. Technol., CoDIT 2020*, pp. 288–293, 9263929, 2020.